



Phytic acid oligomers as bio-based crosslinkers for epoxy and polyol resins

P. Böhm, M. Dornbusch, J. S. Gutmann

Received: 2 March 2023 / Revised: 8 June 2023 / Accepted: 16 June 2023
© The Author(s) 2023

Abstract In recent years, the chemical industry is not only striving to produce the best possible products for various applications, but the new products should ideally be based on renewable resources. The ideal case of “cradle to cradle” is generally not achievable in the coatings industry, as maximizing product life and preventing product degradation in the environment is usually one of the main goals of the coatings industry. Therefore, if the coatings industry wants to act sustainably, its efforts should be focused on renewable raw materials. This paper presents a process that makes the renewable raw material phytic acid easily accessible for conventional epoxy and polyol resin coating systems through hydrophobization- and oligomerization. Phytic acid, as a phosphorus reservoir in plants and with beneficial properties for corrosion protection and as a flame retardant, could be a new base for various coatings. In this work, a simple one-pot oligomerization of phytic acid with green mono- and difunctional alcohols is investigated. The aim of this work is to create a phytic acid hardener system

based on renewable raw materials that can produce coatings with solvent-based epoxy and polyol binders as well as water-based epoxy binders. The successful reaction was observed by infrared, $^1\text{H-NMR}$, and $^{31}\text{P-NMR}$ spectroscopy and the acid equivalent weight was determined by conductivity titration. The renewable curing agent was then used equivalently with different binder systems to prepare coatings. Crosslinking and glass transition temperature were monitored using oscillatory rheology. The coatings were applied to glass plates and the pendulum hardness was measured. A simple heating test followed by $^{31}\text{P-NMR}$ and IR spectroscopy was also performed to demonstrate the stability of phytic acid under reaction conditions.

Keywords Phytic acid, Crosslinking, DMTA, Renewable

Introduction

Phytic acid (PA), a hexakis phosphate ester of myo-inositol (Fig. 1), is a well-known, non-toxic, renewable substance that can be obtained from various plants such as cereal grains, nuts, oilseeds and tubers, etc.¹ Currently, phytic acid is mainly produced as a by-product in the production of bioethanol.² Phytic acid can form stable complexes with various metals.³ Because of this ability, phytic acid is often declared a so-called anti-nutrient in food and feed as it reduces the bioavailability of different trace elements and can deactivate specific enzymes in the digestive track.¹ It can only be digested by ruminants and is therefore indigestible to other livestock and humans.⁴ If it is possible to extract phytic acid without compromising feed quality, it may be one of the few plant molecules that is not in direct competition between the feed/food and chemical industries. However, medical research suggests that phytic acid has various preventive and

Supplementary Information The online version contains supplementary material available at <https://doi.org/10.1007/s11998-023-00827-x>.

P. Böhm, M. Dornbusch (✉)
Department of Chemistry and Institute for Coating and Surface Technology ILOC, Hochschule Niederrhein University of Applied Sciences, Adlerstr. 1, 47798 Krefeld, Germany
e-mail: michael.dornbusch@hs-niederrhein.de

P. Böhm
e-mail: patrick.boehm@hs-niederrhein.de

J. S. Gutmann
Physical Chemistry and CENIDE, Department of Chemistry, University of Duisburg-Essen, Universitätsstr. 2, 45141 Essen, Germany
e-mail: jochen.gutmann@uni-due.de

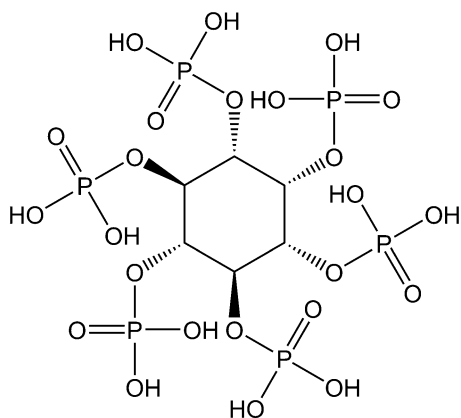


Fig. 1: Myo-inositol hexakisphosphate (phytic acid)

therapeutic effects against tumors in the digestive tract. Additionally, in studies with rats, phytic acid shows beneficial properties against diabetes.^{1,5} Phytic acid has several beneficial properties for the coatings industry. Due to the excellent chelating properties of phytic acid, it can greatly contribute to corrosion protection in coatings.^{6–10} Other publications focus on the flame-retardant properties of phosphates and found these beneficial properties also in coatings and modified natural polymers containing phytic acid.^{11–14} Nitrogen containing molecules could be used to improve the fire-retardant properties further.¹⁵ In this work, we aim to generate easy to use phytic acid oligomers to create crosslinked resins, which can be used with solvent- and water-based systems. To achieve this goal, we need to reduce the free acid functionality of phytic acid, through hydrophobization and generate oligomers. A simple synthesis route without harmful substances or halogens is the direct esterification of phytic acid. This method is not recommended for phosphorus acid but works relatively easily with phytic acid.¹⁶ In addition, we have found that we can use this synthesis to generate phytic acid hardeners in a one-pot reaction. Some publications claim that phytic acid undergoes autohydrolysis at temperatures around 120°C.¹⁷ Therefore, thermal stability under reaction conditions was also tested in this work. The network formation with commercially available products should be done via the residual acid functionality of phytic acid.

Experimental

Analytical methods

The ¹H-, ¹³C-, and ³¹P-NMR spectra were recorded with a Bruker AV NEO 400 NMR (400 MHz) and the samples were dissolved in D₆-DMSO.

IR spectra were measured using a Bruker Vertex 70 (4000–375 cm⁻¹) with ATR and a resolution of 4 cm⁻¹.

The Modular Compact Rheometer MCR 102 from Anton-Paar was utilized to measure relative values of

storage and loss modulus and to determine the glass transition temperature after network formation. A single time plate-plate system with a gap of 1 mm and a diameter of 25 mm was used.

The samples were prepared for the rheological measurements using the DAC 150 1.FV Speedmixer from Hausschild GmbH.

The equimolar mass of the synthesized products was determined using conductivity titration and pH-titration with phenolphthalein. The Touch 900 with the 856-conductivity module from Metrohm was used.

About 0.2 g of the product were dissolved in a mixture of water and ethanol (30:70) and titrated with 0.5 mol/L KOH in ethanol. For the pH titration, three drops of 0.1% phenolphthalein in ethanol was added.

In accordance with DIN EN ISO 1522, DIN EN ISO 11664, DIN EN ISO 2813, DIN EN ISO 13523-11, and DIN EN ISO 2409, the application properties of the coatings were measured with the following equipment: BYK spectro guide sphere gloss; BYK micro-TRI-gloss; BYK crosshatch kit (glass) and the Koenigspendel from Erichsen, respectively.

Materials

Phytic acid (PA) was obtained from Acros Organics B.V.B.A 50% in water. It was then concentrated to about 80% using a rotary evaporator (40–60°C; 70–30 mBar). For IR analysis, it was further concentrated to 84% (60°C; 30–23 mBar). Dodecan-1-ol ≥98 % was purchased by Roth GmbH. Octane-1,8-diol, n-butyl glycidyl ether, phenolphthalein (1% in ethanol) and the different solvents (toluene, methanol, and butanone) were purchased from Sigma-Aldrich and used without further purification. Also, 0.5 mol/L KOH in ethanol, dibutylphosphate, tributylphosphate and butyl phosphate (mixture of mono and diesters) were purchased from Merck. 3-Phenyl-1-propanol 99% was purchased from Thermo Fischer Scientific. p-Phenylenedimethanol >99% was purchased from Tokyo Chemical Industries. From Allnex GmbH, the commercially available hydroxy functional acrylic resin (Macrynal® SM 500/60X) and the two epoxy systems Beckopox® 387w/52WA and the Beckopox® 301/75X were used. Maprenal® MF800/551B and MF920/75W was purchased from Prefere Resins Holding GmbH. For the pigment paste experiments, Bayferrox 130 M from LANXESS was used. Glass plates (10 × 20 × 0.3 cm³) were purchased from Rocholl GmbH.

Synthesis

PA-ester 1 (phytic acid + 2 dodecan-1-ol)

To begin, 40 mmol Dodecan-1-ol was added to 80 mL toluene in a 250 mL round neck flask, with an overhead stirrer, a dean-stark water separator with

cooler and a dropping funnel. Then, 20 mmol phytic acid (80%) was weighted in the dropping funnel and 20 mL toluene was added to the funnel. To prevent material from escaping through foam, a glass pipe with glass wool was installed in front of the water separator. The oil bath was heated to 160°C, and phytic acid was added slowly 15 min after reflux was reached. After adding the phytic acid within 15–30 min, the reaction was boiled at reflux for 12 h or until no more water was separated. The toluene phase was separated from the non-reacted crystalline phytic acid phase.

Conversion: 24% M_{eq} : 82 g/eq

$^1\text{H-NMR}$ (400 MHz, $\text{D}_6\text{-DMSO}$, d, ppm): 0.85 (t, $J=6.8$, $-\text{CH}_3$); 1.24 (m; $-\text{CH}_2(\text{lauryl-chain})$); 1.39 (qint, $J=6.4$, $-\text{O}-\text{CH}_2-\text{CH}_2-[\text{CH}_2]_{\text{lauryl-chain-}}$); 1.54 (qint, $J=6.6$, $\text{P}-\text{O}-\text{CH}_2-\text{CH}_2-[\text{CH}_2]_{\text{lauryl-chain-}}$); 2.50 (qint, $\text{D}_6\text{-DMSO}$); 3.36 (t, $J=6.5$, $\text{H}-\text{O}-\text{CH}_2-\text{CH}_2-$), 3.8 (multi, $\text{P}-\text{O}-\text{CH}_2-\text{CH}_2-$)¹⁸

$^{31}\text{P-NMR}$ (400 MHz, $\text{D}_6\text{-DMSO}$, ppm): -1.09; -1.15 (phosphate-ester)^{18,19}

IR (resonance in $[\text{cm}^{-1}]$): 3291 (OH), 2954 (asym. stretch CH_3), 2922 (asym. stretch CH_2), 2851 (sym. stretch CH_3/CH_2), 2364 (board stretch P-OH), 1691 (board def. P-OH), 1465 (def. CH_2), 1380 (wagging CH_2), 1200 (stretch P=O), 1124 (P=O), 1013 (asym. stretch P-O-C).^{18,20}

PA-oligomer 1 (theoretical dimer) 50% free POH

The 0.125 mol dodecan-1-ol and 0.0125 mol octane-1,8-diol were added to ~100 mL toluene in a 500 mL four neck flask, with an overhead stirrer, a Dean–Stark water separator with cooler, and a dropping funnel. To prevent material from escaping through foam, a glass pipe with glass wool was installed in front of the water separator. The mixture was heated to 160°C and a light nitrogen flow from the Dean–Stark was applied. Then, 0.025 mol phytic acid was then added per dropping funnel and the nitrogen flow was reversed. The strong foam formation should reduce after 30–60 min. After 80–90% of the theoretical amount of water was collected, the clear yellow solution was separated from the solid byproduct and toluene was removed by rotary evaporator (40–60°C, 70–30 mbar). The synthesis route is shown in Fig. 2.

Conversion: 93% M_{eq} : 252 g/eq

$^1\text{H-NMR}$ (400 MHz, $\text{D}_6\text{-DMSO}$, d, ppm): 0.85 (t, $J=6.0$, $-\text{CH}_3$); 1.24 (m; $-\text{CH}_2(\text{lauryl-chain})$); 1.54 (qint, $J=6.3$, $\text{P}-\text{O}-\text{CH}_2-\text{CH}_2-[\text{CH}_2]_{\text{lauryl-chain-}}$); 2.50 (qint, $\text{D}_6\text{-DMSO}$); 3.86 (multi, $\text{P}-\text{O}-\text{CH}_2-\text{CH}_2-$) 3.94 (multi, $(-\text{CH}-\text{OP}-)$)¹⁸

$^{13}\text{C-NMR}$ (400 MHz, $\text{D}_6\text{-DMSO}$, ppm): 13.98 ($-\text{CH}_3$), 22.19–31.4 (various CH_2), 65.26 (laurylalkylchain- $\text{CH}_2\text{-O-P}$), 65.96 (octandiol-alkylchain- $\text{CH}_2\text{-O-P}$)¹⁸

$^{31}\text{P-NMR}$ (400 MHz, $\text{D}_6\text{-DMSO}$, ppm): -1.05; -1.14; -1.19 (various phosphate esters), -13.32 (polyphosphate)^{18,19}

IR (resonance in $[\text{cm}^{-1}]$): 2961 (asym. stretch CH_3), 2921 (asym. stretch CH_2), 2852 (sym. stretch CH_3/CH_2), 2679 (board stretch P-OH), 2317 (board stretch P-OH), 1652 (board def. $[\text{P}=\text{O}]-\text{OH}$), 1466 (def. CH_2), 1375 (wagging CH_2), 1204 (stretch P=O), 1150 (stretch P=O), 1126 (sym. stretch P=O), 1008 (asym. stretch P-O-C)^{18,20}

PA-oligomer 2 (reduced monoester content)

The acid content of PA-oligomer 1 before the removal of toluene was determined. To begin, 0.162 eq POH from PA-oligomer 1 and 0.129 mol n-butyl glycidyl ether were added to a round bottom flask with cooler. The mixture was then heated to 70°C for 5 h using an oil bath with a magnetic stirrer.

M_{eq} : 708 g/eq

IR (resonance in $[\text{cm}^{-1}]$): 3375 (stretch, OH), 2957 (asym. stretch CH_3), 2922 (asym. stretch CH_2), 2857 (sym. stretch CH_3/CH_2), 1466 (def. CH_2), 1377 (wagging CH_2), 1247 (stretch P=O), 1116 (stretch P=O), 1126 (sym. stretch P-O-C), 1006 (asym. stretch P-O-C)^{18,20}

PA-oligomer 3

The reaction procedure corresponds to that of PA-oligomer 1. The dodecanol is replaced with an equimolar amount of 3-phenylpropan-1-ol. After the evaporation of toluene, a clear, amber colored, highly viscous liquid was obtained.

Conversion: 95.6% M_{eq} : 245.7 g/eq

$^1\text{H-NMR}$ (400 MHz, $\text{D}_6\text{-DMSO}$, d, ppm): 1.28 (m, $J=6$, $-(\text{CH}_2)_4-\text{CH}_2-\text{CH}_2-\text{O}$); 1.54 (m; $-\text{CH}_2-\text{CH}_2-\text{O}$); 1.86 (qint, $J=6.5$ ($\text{O}-\text{CH}_2-\text{CH}_2-\text{CH}_2\text{-aromat}$)); 2.62 (m, $\text{CH}_2\text{-aromat}$); 3.86 (multi, $\text{P}-\text{O}-\text{CH}_2-\text{CH}_2-$); 7.23 (multi, (aromat-H))¹⁸

$^{13}\text{C-NMR}$ (300 MHz, $\text{D}_6\text{-DMSO}$, ppm): 30.98–31.76 (various CH_2); 64.57 and 64.63 (various $\text{CH}_2\text{-O-P}$); 125.33, 125.83, 125.87, 128.34, 128.92, 141.19, and 141.39 (various aromatic CH)¹⁸

$^{31}\text{P-NMR}$ (300 MHz, $\text{D}_6\text{-DMSO}$, ppm): -1.04, -1.34 [phosphate ester]^{18,19}

IR (resonance in $[\text{cm}^{-1}]$): 3085, 3064, 3032 (stretch, C-H); 2937 (asym. stretch CH_2); 2861 (sym. stretch CH_2); 2669 and 2325 (board, stretch P-OH vibration); 1658 (board, def. $[\text{P}=\text{O}]-\text{OH}$); 1600, 1581 (stretch C=C); 1498 (def. CH_2); 1469 (mono substituted aromatic C=C); 1454 (def. CH_2); 1390 (wagging CH_2); 1209–1111 (various stretch P=O); 995 (asym. stretch P-O-C); 478 ($(\text{RO})_2(\text{HO})\text{P}=\text{O}$)^{18,20}

PA-oligomer 4

The reaction procedure corresponds to that of PA-oligomer 3. The octane-1,8-diol was replaced with an equimolar amount of 1,4-benzenedimethanol. After

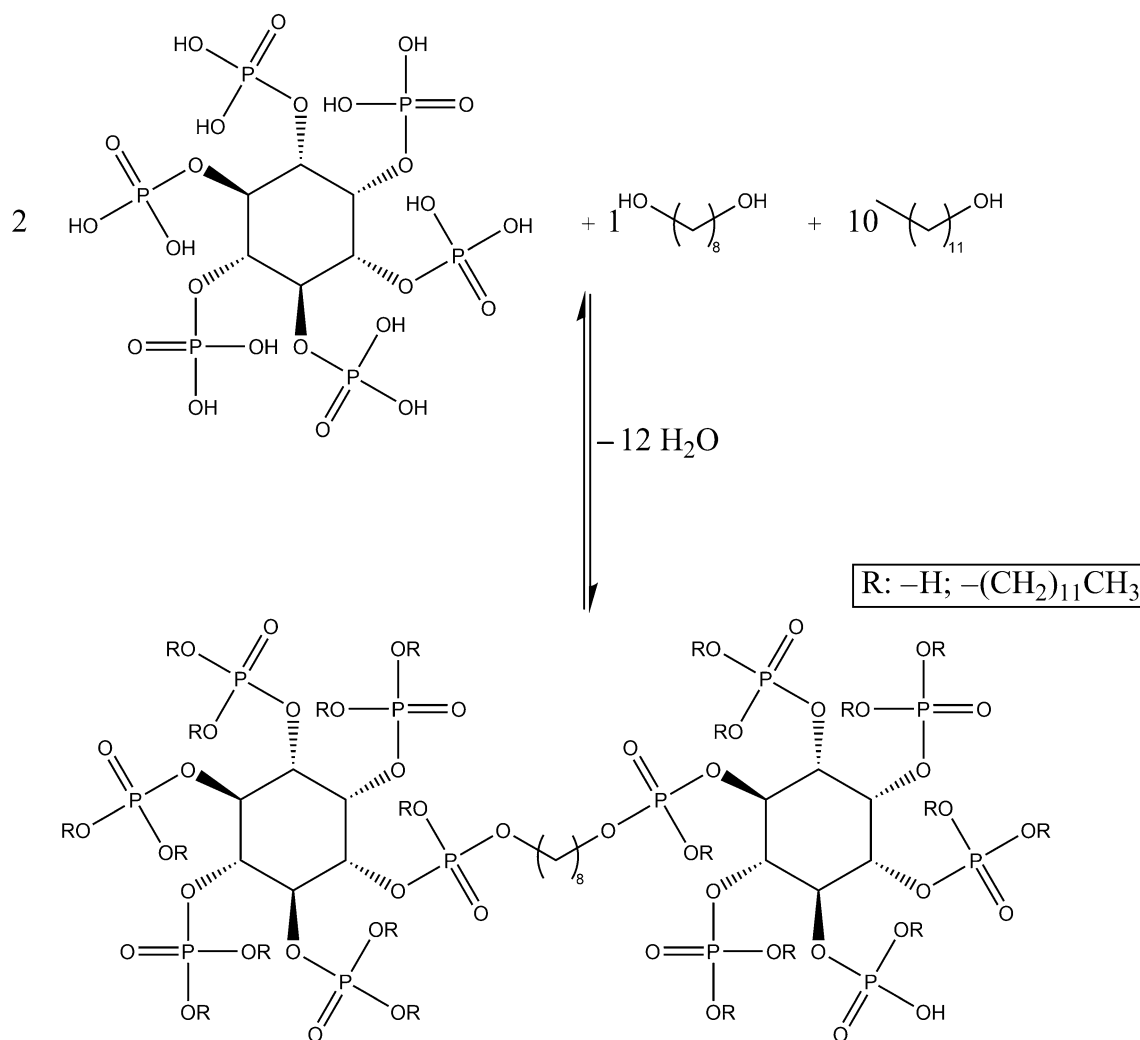


Fig. 2: Theoretical reaction for creation of PA-oligomer 1

the evaporation of toluene, a clear, amber colored, highly viscous liquid was obtained.

Conversion: >99% M_{eq} : 140.1 g/eq

$^1\text{H-NMR}$ (300 MHz, $\text{D}_6\text{-DMSO}$, d, ppm): 1.86 (qint, $J = 6.5$ (O- $\text{CH}_2\text{-CH}_2\text{-CH}_2\text{-aromat}$); 2.62 (m, $\text{CH}_2\text{-aromat}$); 3.86 (multi, P-O- $\text{CH}_2\text{-CH}_2\text{-}$); 7.23 (multi, (aromatic-**H**))¹⁸

$^{13}\text{C-NMR}$ (300 MHz, $\text{D}_6\text{-DMSO}$, ppm): 30.97-31.71 (various CH_2); 64.56 and 64.62 ($\text{CH}_2\text{-O}$); 69.76 (aromat- $\text{CH}_2\text{-O}$); 125.32, 125.83, 125.88, 128.32, 128.91, 141.19, and 141.39 (various aromatic C-H))¹⁸

$^{31}\text{P-NMR}$ (300 MHz, $\text{D}_6\text{-DMSO}$, ppm): - 1.04 & - 1.12 [phosphate ester]; - 13.26 [polyphosphate]^{18,19}

IR (resonance in $[\text{cm}^{-1}]$): 3081, 3060, 3023 (stretch, C-H); 2919 (asym. stretch CH_2); 2863 (sym. stretch CH_2); 2663, 2318 (board, stretch P-OH vibration); 1660 (board, def. $[\text{P}=\text{O}]\text{-OH}$); 1604, 1581 (stretch C=C); 1488 (def. CH_2); 1473 (mono substituted aromatic C=C); 1457 (def. CH_2); 1388 (wagging CH_2); 1209-1114 (various stretch P=O); 997 (asym. stretch P-O-C); 472 ($(\text{RO})_2(\text{HO})\text{P}=\text{O}$)^{18,20}

Synthesis overview

Table 1 shows the theoretical compositions of the diols.

Thermal stability

To check the thermal stability, phytic acid was treated for 12 h under reaction conditions analogous to the PA-oligomer 1 synthesis. Furthermore, it was examined whether changes in the phosphorus NMR are visible when concentrating the phytic acid prior to heat treatment.

Network formation

All formulations were mixed in a 1:1 molar ratio. The formulations are prepared using the Speedmixer. For the rheological measurements, the coatings are applied with a spatula on the single time measurement plate.

The temperature was increased by 2°C per min from 20 to 160°C and then held for 30 min. The shear deformation was constant by 0.1% and the frequency by 10 rad/s. All samples except the melamine formulations were within the LVE-range.¹⁸ To measure the glass transition temperature the cured samples are cooled by 2°C/min to 20°C and then reheated to 100–180°C also by 2°C/min. The deformation and stress were the same as by the curing experiments. To determine the room temperature curing of the epoxy resins, the samples were measured at room temperature for 10 to 48 h. In Fig. 3, theoretical reactions with epoxy or hydroxy-functional resins are shown.²¹

For the application testing, the formulations were applied with a 4-sided draw bar 120 µm gap on glass plates. After 15 minutes at 80°C, the samples were then cured at 160°C for 30 min. The application tests were then carried out in accordance with the relevant DIN norms.

Pigment paste preparation

Pigment pastes were prepared with Bayferrox 130 M and PA oligomers 3 and 4. In each case, an aqueous pigment paste and one based on butyl acetate were prepared. For this purpose, the oligomer was first dispersed in the aqueous phase or dissolved in the butyl acetate. The pigment was then incorporated in a speed mixer (3000 rpm; 1 min) to form a concentration of 66% pigment to 16% PA-oligomer. The pigment pastes were then prepared with the respective epoxy binders and crosslinked either at ambient temperature or by the influence of heat.

Additional measurements

The purchased butyl phosphates were analyzed with IR spectroscopy and ³¹P-NMR spectroscopy.

Results and discussion

Thermal stability

Figure 4 shows the phosphorus NMR of phytic acid 50% and 81% after 12h under reaction conditions. The ppm shift from near zero to ~−0.72 ppm can be explained by the difference in pH. While 50% phytic acid has a pH value of 0.4, 81% has a pH of −0.2. The pH after the reaction could not be measured because the resulting phytic acid was a slightly yellowish, highly hygroscopic, crystalline substance. The shift from higher to lower ppm due to increase in acidity is a well-known phenomenon in phosphorus NMR.²² In addition, the spectra do not show different P species. Conductivity titration of phytic acid after 12 hours

Table 1: Theoretical composition of the PA-oligomers

PA-oligomer number	1	2	3	4
<i>Linker</i>				
Octane–1,8-diol	1	1	1	0
p-Benzenedimethanol	0	0	0	1
<i>Alcohol</i>				
Dodecanol	10	10	0	0
3-Phenylpropan-1-ol	0	0	10	10
Free P-OH groups	12	2	12	12

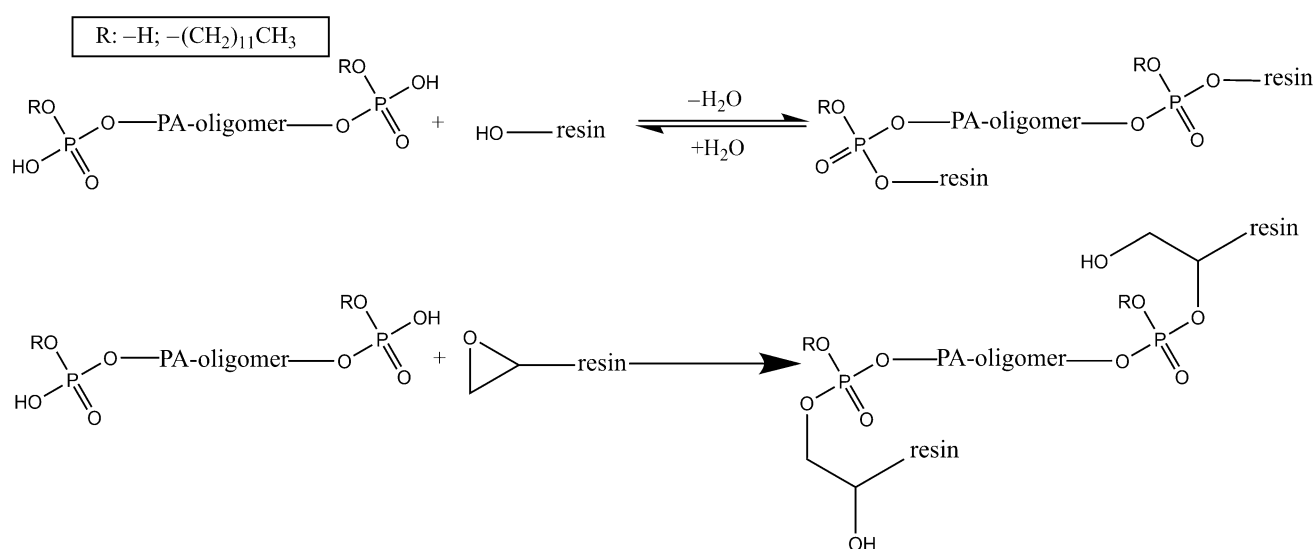


Fig. 3: Possible network formations

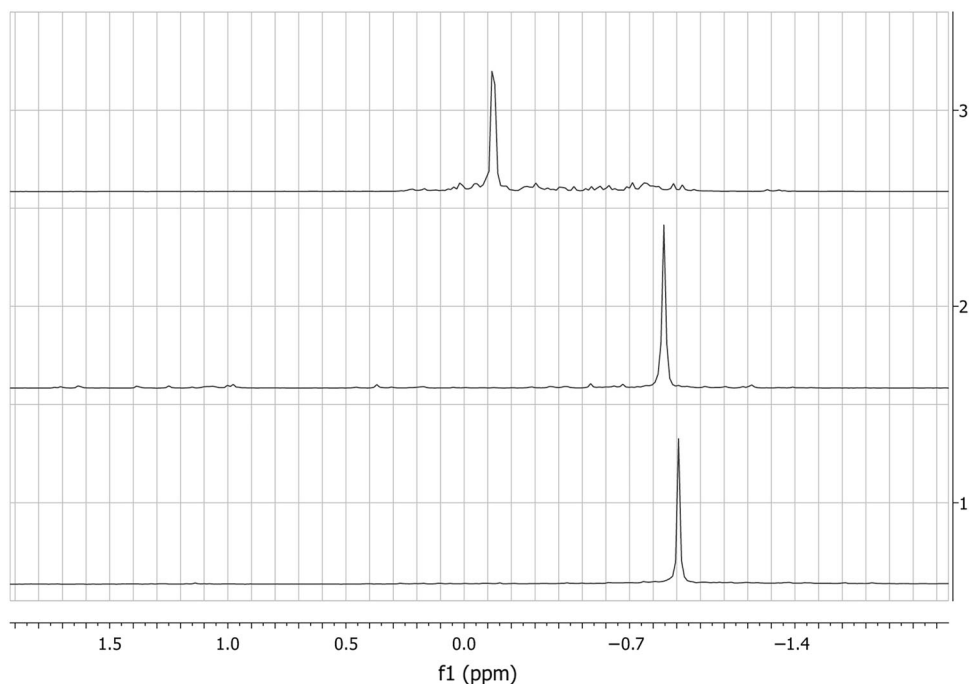


Fig. 4: ^{31}P -NMR spectra of phytic acid 50% (top); 81% (middle); after 12 h under reaction conditions (bottom)

under reaction conditions shows that a concentration of >90% phytic acid can be achieved by this method. After the separation of the phases, we found about 0.5% of unknown chemicals in the toluene phase. These molecules could be a natural pollutant from the extraction process of phytic acid or generated products through the thermal destruction of the phytic acid molecule. Therefore, we can conclude that phytic acid is mostly thermally stable under these conditions. The IR spectra of both phases are shown in the supplemental material (Fig. S1). The solid product corresponds to the concentrated phytic acid spectra.

Synthesis and characterization

In this work a simple method to create phytic acid-oligomers through esterification is presented. The structure cannot be 100% determined, because of the various possibilities to form linear or cyclic structures, with different amount of mono-, di- and tri-phosphate esters. But our results prove that a successful esterification with this method is possible.

In the following IR spectra (Fig. 5), a significant broadening of the sensitive P=O vibration ($1150\text{--}1257\text{ cm}^{-1}$) is clearly visible. The shift and broadening are an indication that the transformation from mono to di-/triesters is successful. Furthermore, if the IR spectra of dibutyl- and tributylphosphate (Fig. S2) are compared, the same shift is visible. The reduced intensity of the three different POH bond vibrations is also an indication that the amount of free POH is greatly reduced. Typical hydroxy vibrations from unreacted

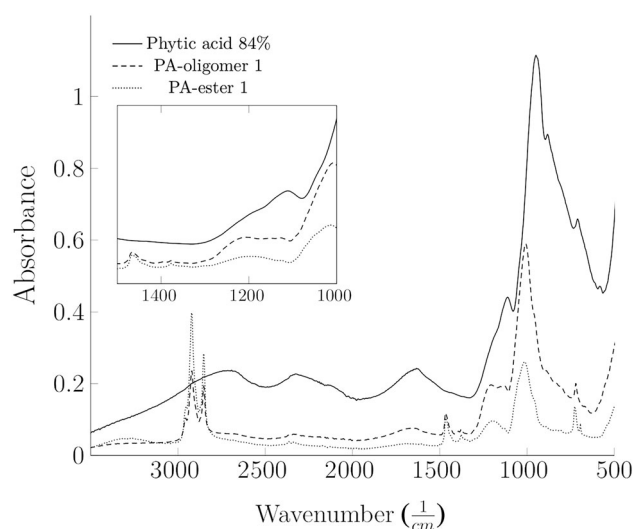


Fig. 5: IR spectra of phytic acid in comparison to PA-oligomer/ester

dodecanol and hydrolyzed phytic acid are not visible for the oligomer synthesis, which is a good indicator that a high conversion is achieved. The same effects are also observed with the other unmodified oligomers (Fig. S3). However, the IR spectrum of the PA-ester 1 still shows a high proportion of free alcohol, which indicates poor conversion.

The comparison of the different ^{31}P -NMR spectra (Fig. 6) of the products shows that we can identify different species of phosphorous atoms. The shift of the signals could be caused by a slightly different pH

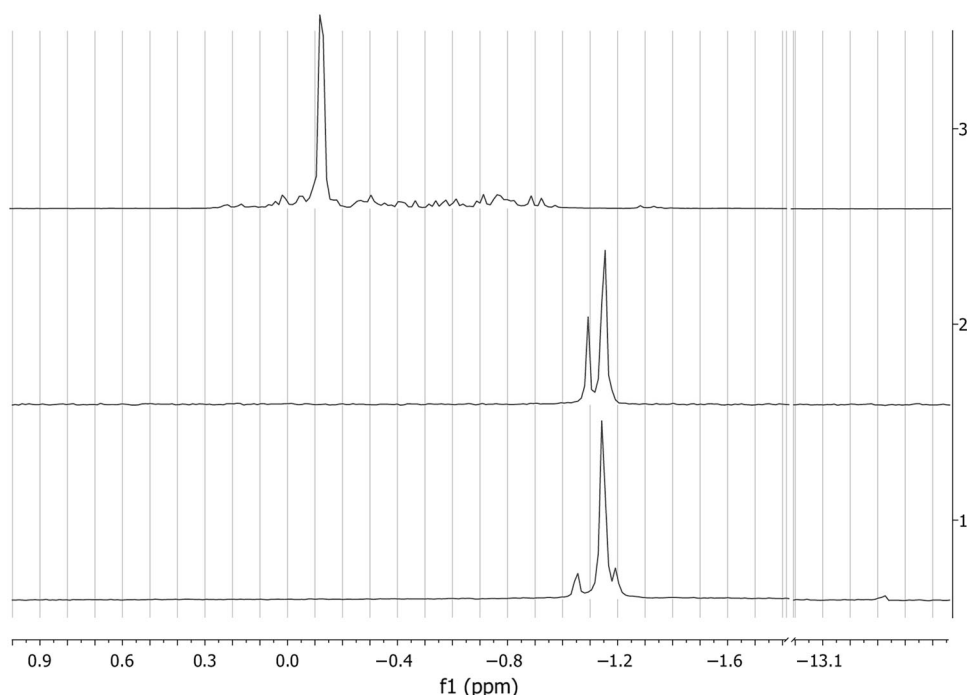


Fig. 6: ^{31}P -NMR spectra of phytic acid 50% (top); PA-ester (middle); PA-oligomer 1 (bottom)

value. The samples were weighed without a neutralization step and therefore contain different numbers of free POH groups. What is clearly recognizable, however, is that we detect only one signal for phytic acid, two signals for the theoretical PA ester, and four signals for the oligomer. This is in line with our expectations, since in the case of phytic acid only monoesters should be present in the case of PA-ester 1 mono- and diester and in the case of PA-oligomer mono-, di- and theoretical triester. The additional signal around -13.3 ppm illustrates that a small number of poly- or pyrophosphates are formed through the reaction. PA-oligomer 3 and 4 display the same effect in the figure, but only oligomer 2 shows a small amount of unreacted the polyphosphate (Fig. S4). The relatively small signal spacing between the different esters is also reflected in the NMR measurements of the different butyl phosphate esters (Fig. S5).

The ^1H -NMR spectrum (Fig. 7) of dodecanol (top) shows that the signals 3 and 5 are significantly influenced through the hydroxy functionality. Therefore, both could be used to check if a reaction occurs. After the reaction, signal 3 shows a shift of $+0.13$ ppm and signal 5 of $+0.42$ ppm. The signal shift to higher ppm is typical for an esterification.¹² We hypothesize that the broadening and multiplet formation of the newly generated signal 6 is produced by the formation of a multitude of slightly different esters. Additionally, the phytic acid C–H signals have nearly the same shift, which results in a poor evaluability of this signal group.

To calculate the conversion rate of the alcohols signals 3 and 4 were compared. The conversion of the

alcohols was significantly higher (93%) for the oligomer than for the PA-ester 1 ($\sim 24\%$).

If we compare the spectra of PA-oligomers 3 and 4 (Fig. S6), we can see that the line broadening is much stronger than in the syntheses with dodecanol. One possible reason for this is that the alcohols used have a significantly shorter carbon chain, and the repetition of the phenyl component produces a line broadening effect similar to that of the repeating units of polymers.²³ The conversion was determined from the signal of the second methylene group between the unreacted and the converted phenyl propanol. In the case of PA-oligomer 4, no more free alcohol could be detected, so that a conversion close to 100% is assumed.

To further prove that this was a true esterification and not a transesterification between dodecanol and phytic acid, a conductometric titration was performed. The resulting equivalent weight should be increased in comparison to the equivalent weight of pure phytic acid. PA-oligomer 1 has an equivalent weight of 252 g/eq (Fig. 8), which is about 97% of the theoretically calculated value of 259 g/eq. To prove that a further reaction with epoxy was also successful, the equivalent weight of PA-oligomer 2 was also determined with a value of 707.4 g/eq. The amount of free unreacted alcohol was included in the calculation. An equivalent mass of 86.25 g/eq was determined for the dry product of PA-ester 1. This corresponds to approximately 4 units of lauryl alcohol per phytic acid.

We assume that the reaction proceeds in two repetitive steps (Fig. 9). First, an intra- or intermolecular phosphorus anhydride is formed by the elimination of water. This step is probably reversible and the

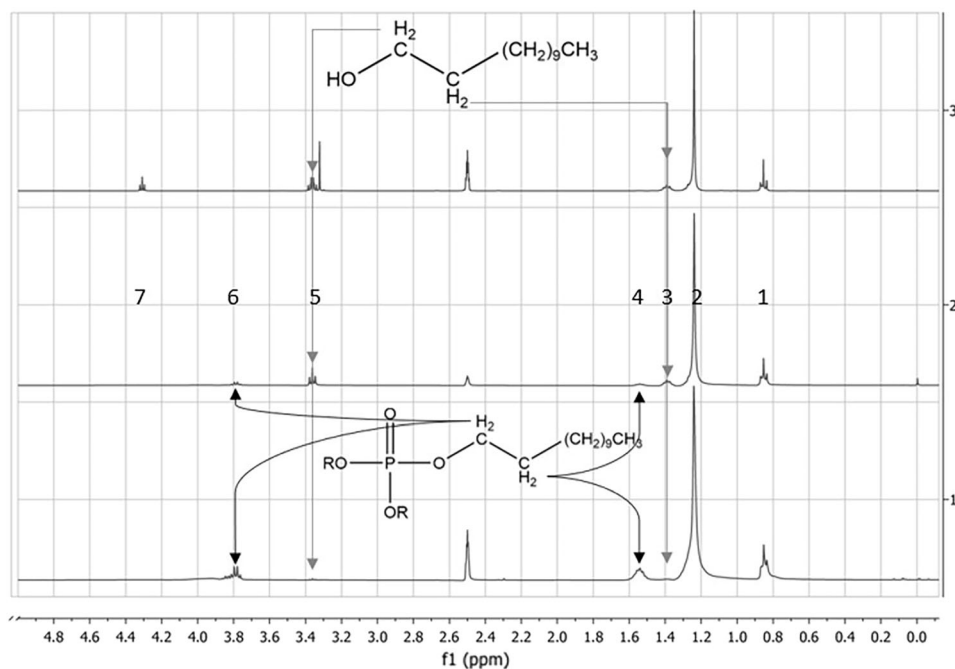


Fig. 7: $^1\text{H-NMR}$ spectra: dodecanol (top); PA-ester 1 (middle); PA-oligomer 1 (bottom)

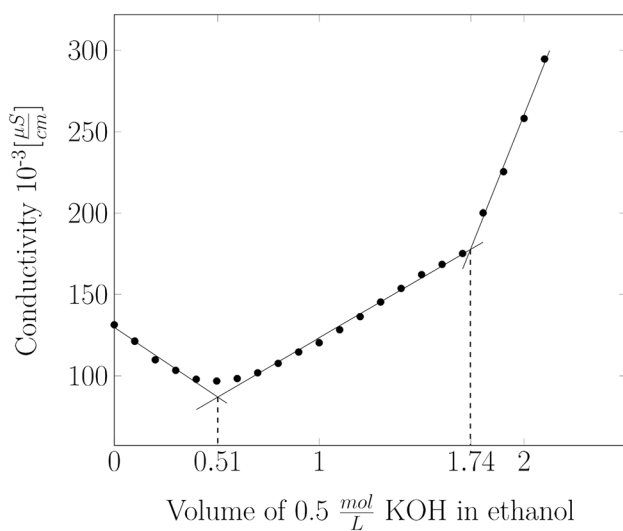


Fig. 8: Conductivity titration of PA-oligomer 1

newly formed anhydride is decomposed if water is present in the environment. The next step occurs at the toluene, phytic acid surface. The alcohol functionality attacks the phosphorus atom, leading to multiple electron transfers and finally to the formation of the new ester. The newly formed PA ester has a typical surfactant structure and the weak to strong foam formation during the reaction is further evidence that the proposed molecule is formed. In the next stage of the reaction it is important, if difunctional alcohol is available or not. We suggest that the high difference of the conversion rates between PA-ester and

PA-oligomer could be explained through the formation of micelles. Unreacted phytic acid is trapped in the micelles and cannot react further. Coalescence of the micelles and evaporation of the water results in various phytic acid crystal formations (Fig. S7). During this process, hollow structures can form which are filled with toluene and unreacted alcohol. The crystals are extremely hydrophilic and only for a few minutes stable, if exposed to air. On the other side, if difunctional alcohol is present, the foam formation is reduced over time and instead of a significant crystal phase a clear toluene/product phase is generated. A possible explanation for this effect could be the prevention of micelle formation by the diol components. The reaction with the diol and further reaction with a second phytic acid leads to a significant enlargement of the molecule, which is presumably sterically no longer able to form effective compact micelles and is thus unable to protect free phytic acid from unreacted alcohol.

Network formation

The curing of the various samples was observed using oscillation measurements (Figs. 10, 11, 12; Fig. S8, 9). All samples show a strong and stable increase of the storage modulus which is classical for network formations. Since a plate-plate system was used, the solvent of the samples could not evaporate easily. This results in an unusual progression at the beginning of the different network formation. The gel point is defined by the build-up of higher structures in the polymer matrices and its value is determined by the point at

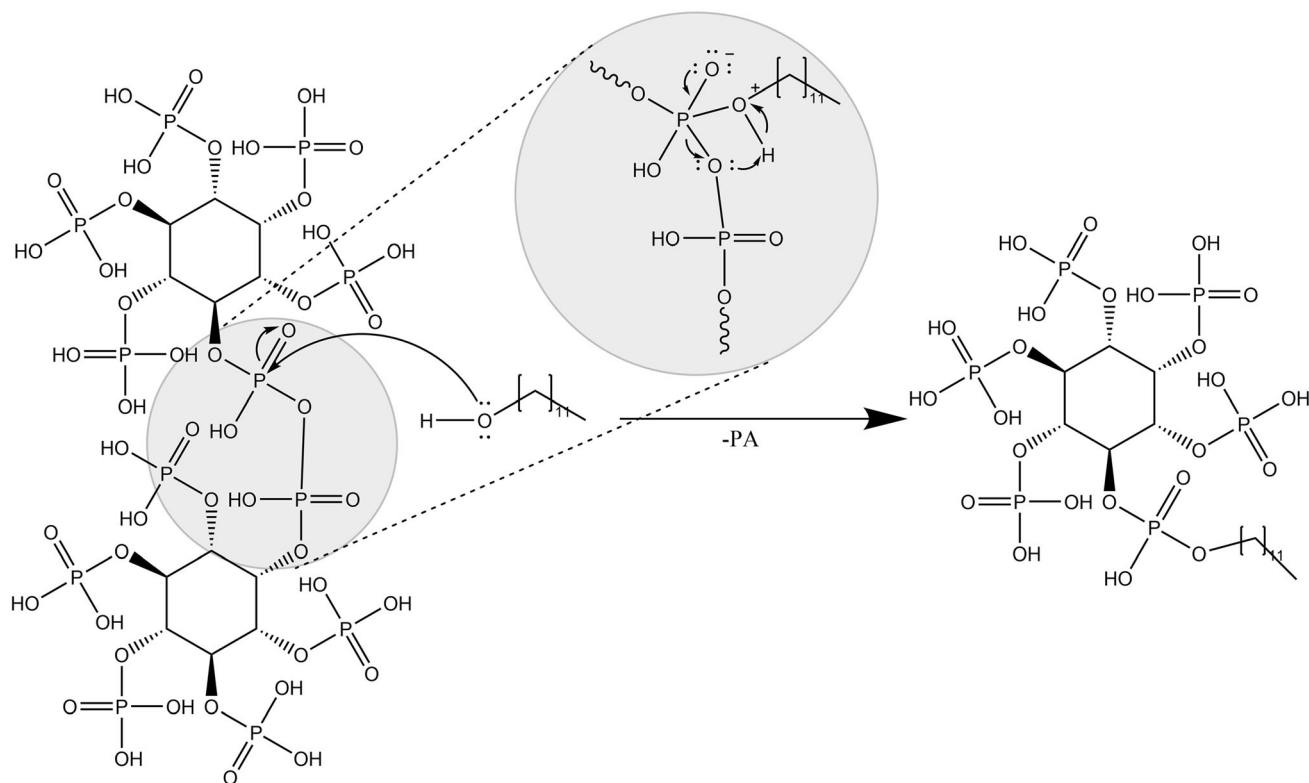


Fig. 9: Proposed reaction mechanism

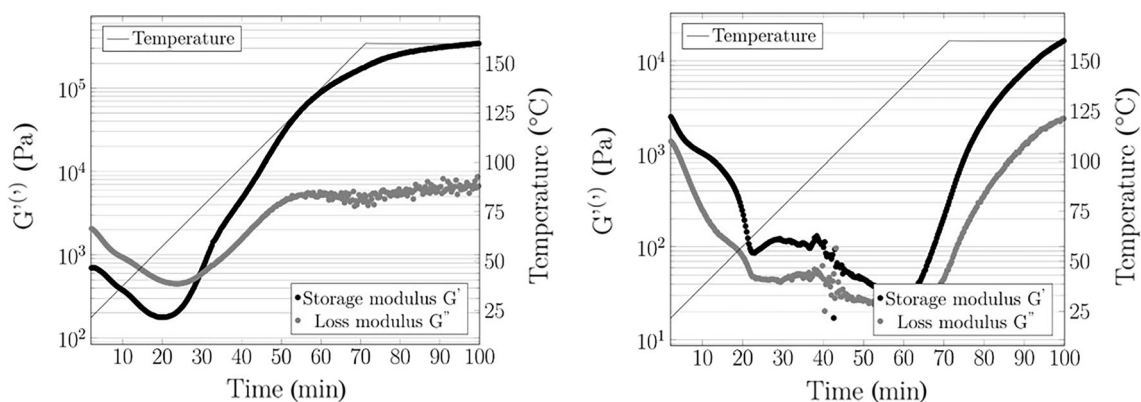


Fig. 10: Network formation: PA-oligomer 1 with Beckopox™ 301/75X (left); Beckopox™ EP 387w/52WA (right)

which the storage modulus exceeds the loss modulus. It is also the minimum temperature required for curing. A second indicator for the successful curing is the glass transition temperature. The glass transition temperature is determined using the maximum of the loss modulus. All measurable samples show typical behavior of polymer networks before and after the glass temperature (Fig. S10). Only the sample with Macrynal® SM500/60X shows a small rubbery elastic region shortly after the glass transition temperature. The melamine samples could not be measured without destruction of the internal structures (sample exceeds

LVE-range) therefore, a glass transition temperature could not be determined. Nevertheless, a successful network formation can be assumed since the storage modulus rises significantly above the loss modulus before exceeding the LVE.²⁴ To further demonstrate network formation, extraction experiments were performed with water, methanol, and butanone, in which phytic acid could not be extracted. This proves that the oligomers not only act as a catalyst but are also a part of the newly created network. Additionally, network formation experiments by ambient temperature with

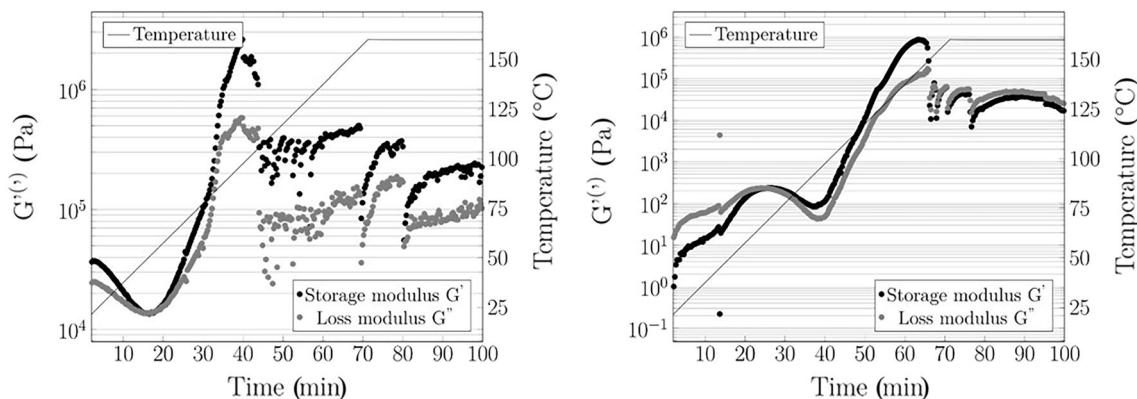


Fig. 11: Network formation: PA-oligomer 1 with Maprenal® MF 920/75WA (left); Maprenal® MF 800/551B (right)

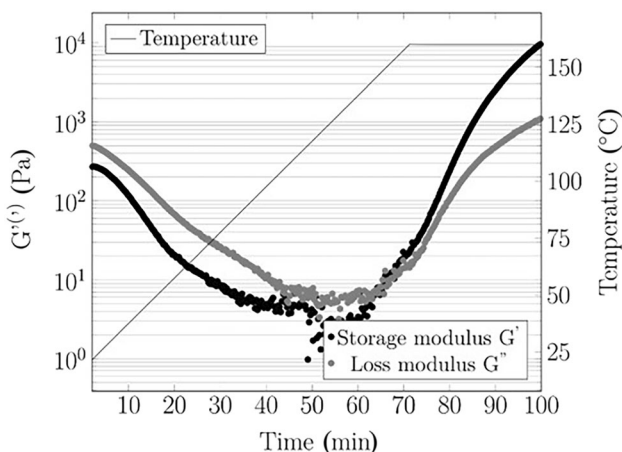


Fig. 12: Network formation PA-oligomer 1 with Macrynal® SM 500/60X

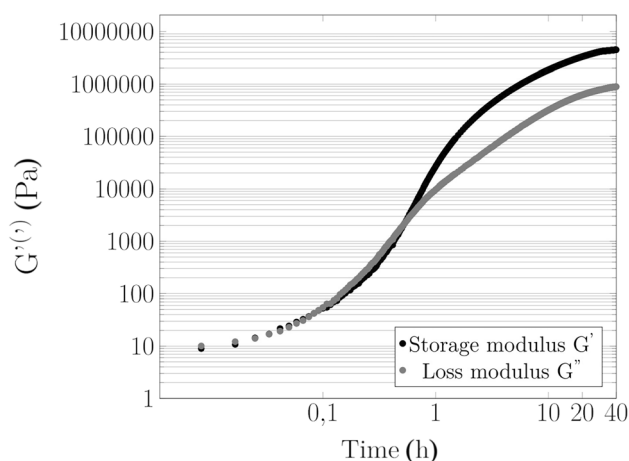


Fig. 13: Network formation PA-oligomer 4 [20°C] with bisphenol a diglycidyl ether

bisphenol A diglycidyl ether and PA-oligomer 3 and 4 were successfully conducted (Fig. 13; Fig. S.11).

Application testing

For application testing the products were equimolar mixed and with a 120 μm 4-sided applicator frame applied to glass plates and subsequently cured. To improve the surface of the water-based systems the PA-oligomer 1 was dispersed in 50% water and then mixed with the water-based systems. In Table 1 the application data are summarized. The theoretically high network density due to the high functionality of the phytic acid oligomers is reflected in the high pendulum hardness. The strong difference between PA-oligomer 1, 3, and 4 could be explained through the different building blocks. The glass transition temperature across the different oligomers is relatively similar, which could be explained by the relatively large binder systems compared to the different PA oligomers, which thus have a higher influence on the glass transition temperature (Table 2). The relatively low

glass transition temperature of Beckopox 387w/52WA and Macrynal can be explained by the water present or formed in the respective samples. Due to the plate-plate geometry of the rheometer, this water cannot evaporate and thus interferes with the crosslinking reaction. This leads to an apparently lower Tg than with a sample where the water can evaporate freely.²⁵ The gel point in this test is strongly influenced by the solvent since outgassing at the rheometer is hindered. The actual gel point of the epoxies is therefore probably significantly higher, especially for the water-based systems. The slightly poorer adhesion of oligomer 1 could be explained by the dodecanol carbon chains in the epoxies, which provide lower interaction forces with the polar surface compared to the shorter aromatic alcohols of oligomers 2 and 3.²⁶ In addition, the steric of PA oligomer 1 and the reaction mechanism of crosslinking in the case of OH acrylate could also have an influence on the adhesion strength. The MEK stability tests show that the epoxy systems crosslinked with the oligomers exhibit excellent solvent stability. In contrast, the crosslinked OH acrylates exhibit significantly poorer to virtually no solvent

Table 2: Application data of various PA-oligomers with different binders

Binder PA-oligomer type	Macrynal® SM 500/60X			Beckopox™ 301/75X			Beckopox™ 387w/52WA		
	1	3	4	1	3	4	1	3	4
<i>160°C-curing</i>									
Pendulum hardness	86	136	137	66	171	171	74	114	89
Gel point[°C]	146	160	160	76	60	30	< 20	158	144
Tg[°C]	45	47	54	61	62	67	38.7	47	38
Crosscut (2 mm)	5	0	0	2	0	0	1	0	0
<i>MEK double rub test</i>									
25 double rubs	Failed	Passed	Passed	Passed					
50 double rubs	N/A	Failed	Failed	Passed					
100 double rubs	N/A	N/A	N/A	Passed					

Table 3: Color measurement of dried pigment pastes

	PA-oligomer 3 pigment paste		PA-oligomer 4 pigment paste	
	Water-based	Solvent-based	Water-based	Solvent-based
L*[65 K;10°]	38.6	37.7	37.9	37.7
a* [65 K;10°]	19.2	20.5	18.6	19.8
b* [65 K;10°]	9.9	10.6	9.9	9.9
ΔE	1.7		1.2	

stability. This indicates a very low degree of crosslinking, which can be explained on the one hand by the steric nature of oligomer 1 and on the other hand by the crosslinking reaction. Crosslinking by esterification has the disadvantage that the water formed cannot always escape completely from the film. This can lead to a lower conversion or even to the cleavage of the ester bonds. Overall, the data show that the oligomers are suitable for the crosslinking of industrial OH acrylate and epoxy resins and, especially in the case of epoxides, for the preparation of coatings with good application properties.

Dispersing and hardening agent

No optimization of the pigment paste has yet been carried out in the tests, which are merely intended to serve as proof-of-concept as to whether the PA-oligomer can fulfill the functions of a hardener and dispersant at the same time. The pigment pastes are stable for at least 3 weeks.

The color measurements of the dried pigment pastes in Table 3 show that the difference between both colors is relatively small with a ΔE value of 1.7 and 1.2, respectively; only trained eyes will notice a difference. However, this is only a proof of concept since all pastes were dispersed under the same relatively simple conditions.

Table 4 shows measurement results of the cured coatings. The water-based systems have a lower pendulum hardness in both room temperature drying and thermal curing, which could indicate that a reaction between water and a part of the epoxy binder occurs. The gloss value of the air-dried coatings is in most samples higher than the cured samples, which is probably because no solvent mixture was used to optimize the curing process. As a result, the solvent escapes too quickly during curing, resulting in a rougher surface. The similar $L^*a^*b^*$ values of the experiments indicate that the water- and solvent-based pigment pastes are similar in their dispersion properties. Overall, the creation of a pigment paste and the crosslinking could be successfully carried out with the PA-oligomers.

Conclusions

A simple esterification at temperatures around 120°C of phytic acid with different alcohols is possible. All analytical methods prove a successful reaction of the PA and a formation of PA esters. Phytic acid is almost completely stable under the used reaction conditions. The reaction of the PA esters occurs through the formation of internal or external pyrophosphates, which are attacked by the hydroxyl functionality of the alcohols and lead to ester formation. All reactants are renewable, which results in a 100% green hardener

Table 4: Application data of PA-oligomer/ Bayferrox 130 M pigment paste with different binders

Binder	PA-oligomer 3		PA-oligomer 4	
	Water-based Beckopox™ 387w/52WA	Solvent-based (BuAc) Beckopox™ 301/75X	Water-based Beckopox™ 387w/52WA	Solvent-based (BuAc) Beckopox™ 301/75X
<i>160 °C curing</i>				
Pendulum hardness	53	117	21	107
Gloss [20°;60°85°]	0.5; 6; 59	24; 71; 82	5; 39; 71	52; 78; 86
L*[65 K;10°]	36.8	36.9	35.5	37.3
a* [65 K;10°]	20.3	22.6	23.3	22.9
b* [65 K;10°]	13.46	13.1	13.5	14.3
<i>Ambient temperature curing</i>				
Pendulum hardness	33	60	39	46
Gloss [20°;60°;85°]	49; 82; 91	63; 91; 94	31; 71; 81	52; 78; 86
L*[65 K;10°]	36.1	37.0	36.9	37.5
a* [65 K;10°]	22.8	22.3	23.0	23.1
b* [65 K;10°]	13.3	12.7	14.3	14.3

system capable of forming networks with various commercially used systems. Reaction with monofunctional epoxy systems can further reduce the amount of free phosphoric acid groups and could be used to optimize PA systems. We have shown that phytic acid oligomers can be used as a dispersing and hardening agent in water- and solvent-based systems for Bayferrox 130 M. If phytic acid curing agents demonstrate their ability to improve corrosion protection and flame-retardant properties, it is possible that phytic acid-based coatings will form a new branch of renewable coating systems. Further work will produce coatings with even better properties suitable for industrial use.

Funding Open Access funding enabled and organized by Projekt DEAL.

Conflict of interest The authors declare that they have no conflict of interest.

Open Access This article is licensed under a Creative Commons Attribution 4.0 International License, which permits use, sharing, adaptation, distribution and reproduction in any medium or format, as long as you give appropriate credit to the original author(s) and the source, provide a link to the Creative Commons licence, and indicate if changes were made. The images or other third party material in this article are included in the article's Creative Commons licence, unless indicated otherwise in a credit line to the material. If material is not included in the article's Creative Commons licence and your intended use is not permitted by statutory regulation or exceeds the permitted use, you will need to obtain permission directly from the copyright holder. To view a copy of this licence, visit <http://creativecommons.org/licenses/by/4.0/>.

References

- Oatway, L, Vasanthan, T, Helm, JH, "Phytic Acid." *Food Rev. Int.*, **17** (4) 419–431. <https://doi.org/10.1081/FRI-100108531> (2001)
- Reis, CER, Rajendran, A, Hu, B, "New Technologies in Value Addition to the Thin Stillage from Corn-to-Ethanol Process." *Rev. Environ. Sci. Biotechnol.*, **16** 175–206. <https://doi.org/10.1007/s11157-017-9421-66> (2017)
- Marolt, G, Gricar, E, Philar, B, Kolar, M, "Complex Formation of Phytic Acid with Selected Monovalent and Divalent Metals." *Front. Chem.*, <https://doi.org/10.3389/fchem.2020.582746> (2020)
- Gupta, RK, Gangoliya, SS, Singh, NK, "Reduction of Phytic Acid and Enhancement of Bioavailable Micronutrients in Food Grains." *J. Food Sci. Technol.*, **52** (2) 676–684. <https://doi.org/10.1007/s13197-013-0978-y> (2015)
- Omoruyi, FO, Budiawan, A, Eng, Y, Olumese, FE, Hoesel, JL, Ejilemele, A, Okorodudu, AO, "The Potential Benefits and Adverse Effects of Phytic Acid Supplement in Streptozotocin-Induced Diabetic Rats." *Adv. Pharmacol. Sci.*, <https://doi.org/10.1155/2013/172494> (2013)
- Xiong, C, Li, W, Jin, Z, Gao, X, Wang, W, Tian, H, Han, P, Song, L, Jiang, L, "Preparation of Phytic Acid Conversion Coating and Corrosion Protection Performances for Steel in Chlorinated Simulated Concrete Pore Solution." *Corros. Sci.*, **139** 275–288. <https://doi.org/10.1016/j.corsci.2018.05.018> (2018)
- Tang, F, Wang, X, Xu, X, Li, L, "Phytic Acid Doped Nanoparticles for Green Anticorrosion Coatings." *Colloids Surf. A Physicochem. Eng. Aspects*, **369** (1–3) 101–105. <https://doi.org/10.1016/j.colsurfa.2010.08.013> (2010)
- Zhang, Y, Cui, X-J, Shao, Y, Wang, Y, Meng, G, Lin, X-Z, et al. "Role of Phytic Acid in the Corrosion Protection of Epoxy-Coated Rusty Steel." *ACMM*, **66** (2) 188–194. <https://doi.org/10.1108/ACMM-07-2018-1973> (2019)
- Yang, S, Sun, R, Chen, K, "Self-Healing Performance and Corrosion Resistance of Phytic Acid/Cerium Composite Coating on Microarc-Oxidized Magnesium Alloy." *Chem. Eng. J.*, **428** 131198. <https://doi.org/10.1016/j.cej.2021.131198> (2022)

10. Rausch, W. *Die Phosphatierung von Metallen*. 3rd ed., pp. 92, Bad Saulgau, München: Leuze; Carl Hanser Verlag (Hanser eLibrary) (2005). <https://doi.org/10.12850/97838748031137>
11. Cheng, X-W, Guan, J-P, Yang, X-H, Tang, R-C, Yao, F, “A Bio-resourced Phytic Acid/Chitosan Polyelectrolyte Complex for the Flame Retardant Treatment of Wool Fabric.” *J. Clean. Prod.*, **223** 342–349. <https://doi.org/10.1016/j.jclepro.2019.03.157> (2019)
12. Feng, Y, Zhou, Y, Li, D, He, S, Zhang, F, Zhang, G, “A Plant-Based Reactive Ammonium Phytate for Use as a Flame-Retardant for Cotton Fabric.” *Carbohydr. Polym.*, **175** 636–644. <https://doi.org/10.1016/j.carbpol.2017.06.129> (2017)
13. Wang, D, Wang, Y, Li, T, Zhang, S, Ma, P, Shi, D, et al. “A Bio-Based Flame-Retardant Starch Based on Phytic Acid.” *ACS Sustain. Chem. Eng.*, **8** (27) 10265–10274. <https://doi.org/10.1021/acssuschemeng.0c03277> (2020)
14. Yao, C, Xing, W, Ma, C, Song, L, Yuan, H, Zhuang, Z, “Synthesis of Phytic Acid-Based Monomer for UV-Cured Coating to Improve Fire Safety of PMMA.” *Prog. Org. Coat.*, **140** 105497. <https://doi.org/10.1016/j.porgcoat.2019.10.5497> (2020)
15. Zilke, O, Plohl, D, Opwis, K, Mayer-Gall, T, Gutmann, JS, “A Flame-Retardant Phytic-Acid-Based LbL-Coating for Cotton Using Polyvinylamine.” *Polymers*, <https://doi.org/10.3390/polym12051202> (2020)
16. Krüger, W et al., *Organische Phosphor-Verbindungen*. Stuttgart, New York: Thieme (Methoden der organischen Chemie (Houben-Weyl) 4. Ed., Bd. E 2) (1982), <https://www.thieme-connect.de/products/ebooks/book/https://doi.org/10.1055/b-003-109667>
17. Hull, SR, Gray, JS, Montgomery, R, “Autohydrolysis of Phytic Acid.” *Anal. Biochem.*, **273** (2) 252–260. <https://doi.org/10.1006/abio.1999.4220> (1999)
18. Hesse, M, Meier, H, Zeeh, B, *Spektroskopische Methoden in der organischen Chemie, Thieme*, 8th ed. Georg Thieme Verlag, Stuttgart, New York (2011)
19. Godinot, C, Gaysinski, M, Thomas, O, et al. “On the Use of ^{31}P NMR for the Quantification of Hydrosoluble Phosphorus-Containing Compounds in Coral Host Tissues and Cultured Zooxanthellae.” *Sci. Rep.*, **6** 21760. <https://doi.org/10.1038/srep21760> (2016)
20. Socrates, G. *Infrared and Raman Characteristic Group Frequencies*. Tables and Charts. 3rd ed., Chichester, Wiley (2010)
21. Mischke, P, *Film Formation in Modern Paint Systems*. Hannover: Vincentz Network (European Coatings Tech Files) (2010). www.european-coatings.com
22. Streck, R, Barnes, AJ, “Solvent Effects on Infrared, ^{13}C and ^{31}P NMR Spectra of Trimethyl Phosphate: Part 1: Single Solvent Systems.” *Spectrochim. Acta A: Mol. Biomol. Spectrosc.*, **55** (5) 1049–1057 (1999)
23. Friebolin, H, *Ein- und zweidimensionale NMR-Spektroskopie*. Eine Einführung. 5. Ed. Weinheim: Wiley-VCH (2013). <http://site.ebrary.com/lib/alltitles/Doc?id=10658470>
24. Mezger, T, *Angewandte Rheologie. Mit Joe Flow auf der Rheologie-Straße*, 4th edn. Anton Paar GmbH, Graz (2018)
25. Knospe, P, Neuartige Strukturen und Vernetzungsreaktionen für Beschichtungsstoffe, PhD-thesis, Pages 118f (2023)
26. Goldschmidt, A, Streitberger, H.-J., BASF-Handbuch Lackiertechnik., Münster, Hannover: BASF; Vincentz Network, Pages 390ff (2014)

Publisher’s Note Springer Nature remains neutral with regard to jurisdictional claims in published maps and institutional affiliations.